[30] Proton Conduction through Proteins: An Overview of Theoretical Principles and Applications

By Z. SCHULTEN and K. SCHULTEN

Introduction

The transport of protons across transmembrane proteins is a fundamental feature in many bioenergetic systems, and the elucidation of the molecular mechanisms involved is a challenge to both experimentalists and theoreticians. Two of the more intensively studied proton transport systems are the membrane protein bacteriorhodopsin, which functions as a light-driven proton pump in *Halobacterium halobium (H. h.)*,[1] and the proteolipid of ATPase, which functions as a passive proton conductor.[2] The primary sequences of both systems are known.[2,3] For the proteolipid of ATPase the single-channel conductances have been measured.[4] For bacteriorhodopsin, a low-resolution structure has been obtained[5] and the charge displacements accompanying the active proton transport have been observed.[6] Nevertheless, for both systems the molecular mechanism of the proton transport through the proteins is still unknown. The proton channels are not permeable to Na^+ or other positive ions, implying that the radius of the channel is less than 1 Å and that the transport involves either amino acid side groups, which specifically bind protons, or molecules of bound water. Direct observation of the conduction pathways is difficult since the transport may be realized through very minor motions of the protein backbone and side groups. This has been shown recently for the pump cycle of bacteriorhodopsin by detecting the structural difference of its initial state, Br_{568}, and its M_{412} intermediate state (R. Henderson, personal communication). Furthermore, since only a small number of protons suffice for the translocation and since these protons are only a

[1] For a recent review, see W. Stoeckenius and R. Bogomolni, *Annu. Rev. Biochem.* **51**, 587 (1982).

[2] For a recent review, see J. Hoppe and W. Sebald, *Biochim. Biophys. Acta* **768**, 1 (1984).

[3] Y. A. Ochinnikov, N. Abdulaev, M. Fiegina, A. Kiselev, and N. Lobanov, *FEBS Lett.* **100**, 219 (1979); H. Khorana, G. Gerber, W. Herlihy, C. Gray, R. Anderegg, K. Nihei, and K. Biemann, *Proc. Natl. Acad. Sci. U.S.A.* **76**, 5046 (1979).

[4] H. Schindler and N. Nelson, *Biochemistry* **21**, 5787 (1982).

[5] R. Henderson and P. Unwin, *Nature (London)* **257**, 28 (1975); D. Englemann, R. Henderson, A. McLachlen, and B. Wallace, *Proc. Natl. Acad. Sci. U.S.A.* **77**, 2037 (1980); S. Hayward and R. Stroud, *J. Mol. Biol.* **151**, 491 (1981).

[6] L. Drachev, A. Kaulen, and V. Skulachev, *FEBS Lett.* **87**, 161 (1978); L. Keszthelyi and P. Ormos, *FEBS Lett.* **109**, 189 (1980).

METHODS IN ENZYMOLOGY, VOL. 127

minor fraction of the total charges within the protein, the elementary processes involved may go unnoticed in many observations. These difficulties necessitate that the experimental investigations be supported by theoretical investigations which test the pertinent molecular models by evaluating quantities amenable to observation. This chapter summarizes our attempts to provide observables which are suitable to illucidate the structure and function of biological proton conductors.

Current ideas concerning the passive proton transport, i.e., transport down the electrochemical potential existing across the membrane, are based on a model by Onsager[7] which was developed originally to describe the conduction of protons in ice. This model purports that protons are conducted through transmembrane proteins by means of a linear chain of hydrogen-bridged amino acid side groups and molecules of bounded water. Appropriate side groups are polar residues containing either hydroxyl, carboxylic, amide, or amine groups. A more detailed, but qualitative discussion of the application of Onsager's model to biological systems is given in the recent review by Nagle and Nagle.[8] Recent molecular dynamics calculations[9] and permeability experiments[10] indicate that ions are transported across gramicidin through a linear channel containing 8–10 hydrogen-bonded water molecules. The participation of bound water in the proton transport in ATPase is strongly suggested by the fact that very few polar amino acid side groups are found in the interior of the proteolipids of ATPase which span the membrane and appear to be the protein component mainly responsible for proton conduction in ATPase. However, the passive proton conduction in the F_0 fraction of the transmembrane part of native ATPase requires three protein components.[2,11] From neutron diffraction studies on bacteriorhodopsin[12] one can infer that less than 10 molecules of water are present within the protein, i.e., the proton conduction in bacteriorhodopsin is likely to involve amino acid side groups rather than water.

To characterize the proton transport and, in particular, to separate the dynamics of the few protons and groups within a conductor from motions of the entire protein, we will consider in this chapter the time dependence of the following observables for a hydrogen-bridged conductor consisting of heterogeneous groups[13]: (1) the proton current, (2) the charge displacement within the conductor, (3) the free energy change, and (4) the state of protonation of the conductor groups. These quantities were determined for the following possible, experiments: (1) measurement of the pH dependence of the stationary, voltage-induced proton current; (2) the coupling of the proton transport to alternating electric fields; and (3) the response of the conductor to the injection or ejection of a proton. Each of the above-suggested experiments should give, as our calculations show, certain information about the elementary steps and groups involved in the proton transport. For example, measuring the response of the proton conductor to an alternating electric field, i.e., the frequency dependence of the amplitude and phase shift of the proton current and dipole moment, provides a window to view the internal proton motions such as the jumps of protons between groups and the rotations of the conductor groups. Similarly the relaxation times for the charge displacements observed in bacteriorhodopsin after light excitation can be associated to rate constants for these internal motions.

[7] L. Onsager, *in* "The Neurosciences" (F. O. Schmitt, ed.), p. 75. Rockefeller Univ. Press, New York, 1967.
[8] J. Nagle and S. Nagle, *J. Membr. Biol.* **74**, 1 (1983).
[9] D. Mackay, P. Berens, K. Wilson, and A. Hagler, *Biophys. J.* **46**, 229 (1984).
[10] P. Rosenberg and A. Finkelstein, *J. Gen. Physiol.* **72**, 327 (1978).
[11] E. Schneider and K. Altendorf, *Trends Biochem. Sci.* **9**, 51 (1984).
[12] G. Zaccai and D. Gilmore, *J. Mol. Biol.* **132**, 181 (1979).
[13] A. Brünger, Z. Schulten, and K. Schulten, *Z. Phys. Chem.* **136**, 1 (1983).

Theoretical Model and Observables Calculated[13]

The amino acid side groups together with molecules of bound water are assumed to form a linear hydrogen-bonded conductor spanning the membrane. In thermal equilibrium with the solutions at both sides of the membrane at neutral pH, a conductor composed of identical groups with pK values around 7 contains one proton for each group such that adjacent groups are hydrogen bonded through one proton. The proton transport can then be described in terms of intermediate, thermally activated faults which are schematically presented in Fig. 1. The faults represent deviations from the equilibrium situation arising from either the jump of a proton between groups or from the rotation of a group. The protonation and deprotonation of the conductor end groups, processes which are often rate determining, are not shown. We assume that the energies of faults are additive.

The state of the conductor at any time t is determined by a master equation

$$\frac{d}{dt} P(t) = K(t)P(t) \tag{1}$$

where the component $P_i(t)$ of $P(t)$ is the probability that the ith proton configuration (a particular distribution of protons within the conductor; see Fig. 1) is realized. The off-diagonal elements of the rate matrix K_{ij} are rate constants describing the transition $j \rightarrow i$ between proton configurations j and i as a first-order reaction. The transition can involve, e.g., a jump of a proton between two groups (which would correspond to the

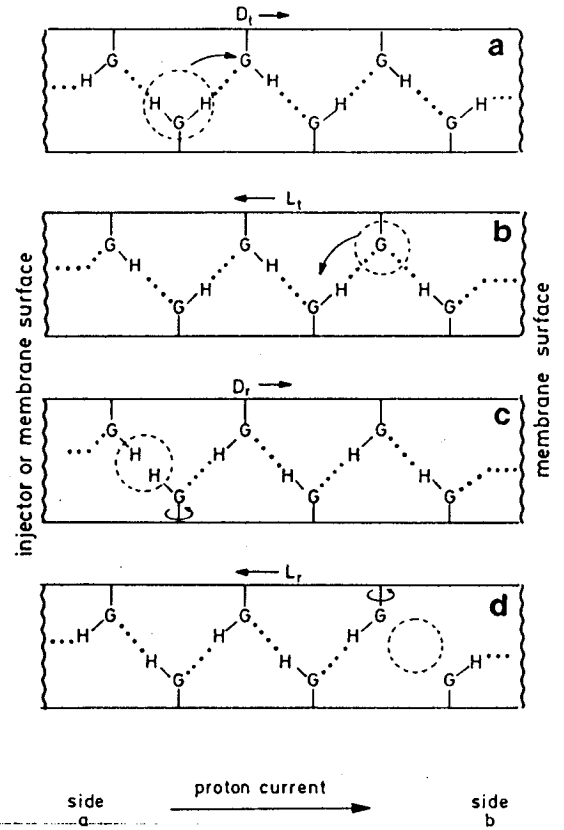

FIG. 1. Elementary steps in the transport of a proton along a transmembrane protein. G are either amino acid side chains or molecules of bounded water that form a linear hydrogen-bonded conductor crossing the membrane. The groups G can be heterogeneous and have at most two states of protonation. The peptide backbones of two adjacent α-helices are represented as straight lines. At equilibrium there is one proton in each hydrogen bond. The proton transport involves the generation and migration of four types of defects, the defects representing deviations from the equilibrium structure: (a) The D_t fault represents a situation with an excess proton on a group; (b) the L_t fault represents a situation with a proton vacancy at a group; (c) the D_r fault represents a situation with two protons between neighboring groups; (d) the L_r represents a situation with no protons between the neighboring groups. The D_t and L_t faults are generated by protonation and deprotonation of the conductor end groups, and their migration involves the jump of a proton from one group to the next. The D_r and L_r faults are generated and moved by rotation of a side group which thereby transports a proton from one side to the other side of the group.

migration of a D_t or L_t fault; see Fig. 1) or to the rotation of a group (which would correspond to the migration of a D_r or L_r fault; see Fig. 1). The conservation of total probability requires the diagonal elements of K to satisfy the relation $K_{ii} = -\sum_j K_{ji}$. The rate constants for motions within the proton conductor obey the Arrhenius law

$$K_{ij} = A_{ij} \exp(-E_{ij}/kT) \tag{2}$$

A_{ij} is a frequency factor of the order 10^{11} sec^{-1}. E_{ij} is the total activation barrier for the transition and includes contributions from time-dependent external and internal electric fields as well as pK differences for heterogeneous groups. The assignment of the values for the rate constants has been discussed.[8,13,14] We assume that the rate constants for the jump of a proton between homogeneous groups is $k_t \simeq 10^{11}$ sec^{-1} and for the rotation of an interior group is $k_r \simeq 10^7$ sec^{-1} for bacteriorhodopsin and $k_r \simeq 10^{10}$ sec^{-1} for the channels connected with the proteolipids of ATPase. The rate constant for the rotation of an end group which introduces a vacancy into the neighboring hydrogen bond $k(\mathrm{O} \rightarrow \mathrm{L_r})$ can be considerably smaller, and for Figs. 2–5 we assumed $k(\mathrm{O} \rightarrow \mathrm{L_r}) \simeq 10^4$ sec^{-1} in the absence of an electric field. pK differences between the groups give rise to an asymmetry in the forward (k_{+t}) and backward (k_{-t}) rate constants for proton jumps, i.e., $k_t \neq k_{-t}$.

The rate constants for protonation and deprotonation of the conductor end groups are

$$\begin{aligned} K_{\mathrm{P}} &= g\kappa_{\mathrm{d}} 10^{-\mathrm{pH}} + k_t'/(1 + k_{-t}'\tau) \text{ (protonation)} \\ K_{\mathrm{D}} &= g\kappa_{\mathrm{d}} 10^{\mathrm{pH}-14} + k_t/(1 + k_{-t}\tau) \text{ (deprotonation)} \end{aligned} \tag{3}$$

The first term describes the diffusion-controlled reaction between the end group and the hydronium (by protonation) or hydroxyl (by deprotonation) ions in the bulk water. g is the probability that the reaction takes place to completion and is of the order 1. κ_{d} is the biomolecular diffusion-controlled reaction rate constant for the ions for which we employed the value 4×10^{10} liter/mol sec in all calculations. κ_{d} may be larger if the diffusion of the ions occurs in two steps: three-dimensional diffusion to the membrane surface followed by lateral diffusion along the surface to the channel entrance.[15] The second term in Eq. (3) describes the transfer of a proton between the end groups (allowing for different states of protonation) and bulk water. $k_{\pm t}(k_{\pm t}')$ are pK-dependent rate constants for the forward and backward transfer. τ is a structural relaxation time for water and is of the order 10^{-11} sec.

[14] Z. Schulten and K. Schulten, *Eur. Biophys. J.* **11**, 149 (1985).
[15] T. H. Haines, *Proc. Natl. Acad. Sci. U.S.A.* **80**, 160 (1983).

Proton Current

The proton current across the right conductor end group is given by the transition fluxes $F_{i \leftarrow j}$

$$J_R = \sum F_{i \leftarrow j} = \sum (K_{ij} P_j - K_{ji} P_i) \tag{4}$$

where the sum is over all transitions $(i \leftarrow j)$ involving protonation of the right end group. The integrated current is then

$$T_R(t) = \int_0^t dt' \, J_R(t') \tag{5}$$

Dipole Moment

The dipole moment of the conductor is given by

$$\mu(t) = \sum_i \mu_i P_i(t) + ed T_R(t) \tag{6}$$

where μ_i is the dipole moment of the ith proton configuration and is defined as the sum of the dipole moments of all protons in the configuration with the reference point taken at the left-hand side. d is the width of the membrane and e is the proton charge. Only the component of the dipole moment in the direction of the conductor is considered.

Free Energy

As a measure of the system's deviation from equilibrium, we also evaluated the change in its free energy

$$\Delta F(t) = kT \sum_i P_i(t) \ln[P_i(t)/P_i^0] = F(t) - F(0) \tag{7}$$

where P_i^0 are the components of the equilibrium distribution defined through the matrix equation

$$KP^0 = 0$$

Application to the Proteolipid of ATPase[13,14]

General Remarks

An important step in understanding the transport of protons in biological systems is the recent measurement by Schindler and Nelson[4] of the conductance of single proton channels formed by the proteolipids of ATPase after reconstitution into planar bilayers. We derived[13,14] a simple

analytical expression for the conductance of a single proton channel in terms of the pK values of the conducting groups and the kinetic constants of the elementary steps and compared the results to the conductances measured. This comparison revealed that the observed conductance is in agreement with a model of a proton channel constructed from bound water and indicated that the hydrogen bonds between the groups are weak, i.e., can be broken on a time scale of 100 psec. This channel provides a most suitable example to introduce the concepts behind a theoretical description of biological proton conduction and, therefore, we will consider it here.

It is generally accepted that at least two proteolipids are required to form a channel and that the aspartic (glutamic) acid residues are a key component of the proton channel. Sequence and structural studies indicate that the aspartic acid residue is located roughly in the middle of the membrane.[2,16] Since the proteolipid appears to be a hairpin α-helix with largely hydrophobic segments crossing the membrane, the two proteolipids may be nested together in order to utilize the largest number of hydrogen-bonding side groups for the proton transport. Hoppe and Sebald[2] have recently suggested that a proton channel could be totally constructed from water molecules that are bound either by the amino acid side groups or by the polar groups of the peptide bonds. Since the exact arrangement is not known, and since it is difficult to differentiate kinetically the transport of a proton by a molecule of bound water from the transport by an organic hydroxyl group as threonine, we will consider the following simple model:

The channel consists of N groups with the center group representing a cluster of one or more aspartic acid side chains. Each group in the channel has two states of protonation and correspondingly two pK values. For aspartic acid the pK values describe the formation of the carboxylate and oxonium ions

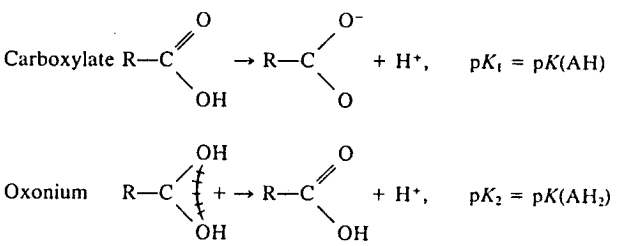

[16] A. Senior, *Biochim. Biophys. Acta* **726**, 81 (1983); A. Senior and J. Wise, *J. Membr. Biol.* 73, 105 (1983).

The other conductor groups (WH) are assumed to be either bound water or polar side groups and their two states of protonation are

"Hydroxyl" $WH_2 \rightarrow W^- + H^+$, $pK_1 = pK(WH)$
"Hydronium" $WH_2 \rightarrow WH + H^+$, $pK_2 = pK(WH_2)$

In analogy to the experimental situation, we will assume in our calculations that the pH values of the solutions on either side of the membrane are titrated symmetrically and that the proton current is induced by a voltage difference applied across the membrane. The mechanism underlying the proton current is revealed by determining which route through the space of proton configurations produces the current. The dominant routes are marked by the largest transition fluxes $F_{i \leftarrow j}$ [see Eq. (4)]. Since the proton transport leaves the conductor unaltered, this process is represented by cycles which connect those proton configurations contributing to the transport and which return to a starting configuration. In most cases, e.g., homogeneous conductors, only a few cycles contribute. The transport connected with the proton channels of the proteolipids of ATP-

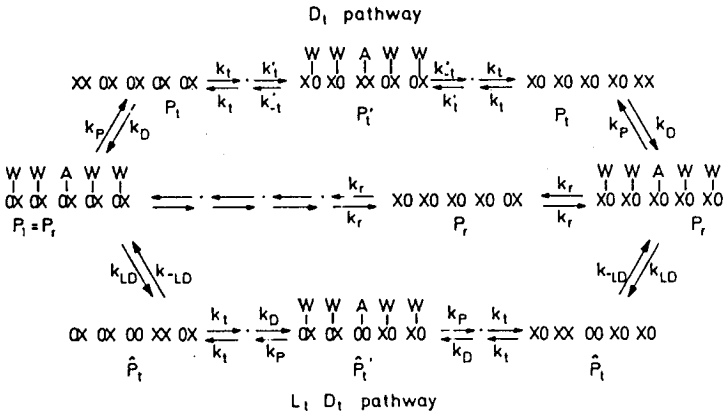

FIG. 2. Kinetic model of the proton channel formed by the proteolipids at ATPase: The center group (A) is assumed to be the carboxylate side group of aspartic acid. The neighboring groups (W) are either molecules of bound water or amino acid side groups. For convenience only five groups are shown. The symbol XO represents the case that a proton (no proton) is situated at one of the two possible binding sites of each group. The rate constants which govern the transitions between the proton configurations, e.g., k_r and k_t where the indexes r and t refer to rotation or jump motion, are shown. P and D denote protonation–deprotonation processes at the end groups and LD the transfer of a proton between the aspartic acid central group and one of its neighboring groups. Two equilibrium proton configurations in the hydrogen-bonded network in which the protons are situated all to the right or all to the left of the groups are shown. Several intermediate configurations denoted by · have been omitted.[14]

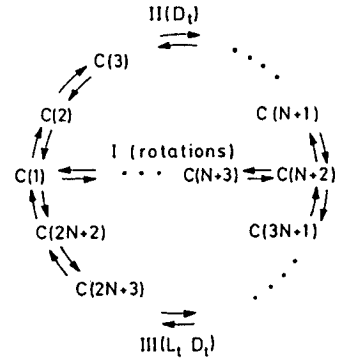

FIG. 3. Schematic representation of the two pathways of proton transport in Fig. 2 for a channel composed on N groups. C(i) denote the individual proton configurations. The resistance attributed to the three unbranched parts of the network is indicated (see text).

ase will involve primarily the series of proton configurations shown in Figs. 2 and 3. The symbols OO, OX, XO, and XX in Fig. 2 represent the four possible protonation states of a single group, i.e., no proton, one proton to the right, one proton to the left, and two protons on either side of the respective group. The symbol OX OX OX OX OX in Fig. 2 represents the equilibrium configuration, denoted by C(1) in Fig. 3, with all protons to the right side of the groups; XO XO XO XO XO represents the other equilibrium configuration, denoted by C(N + 2), with all protons to the left-hand side of the groups. The symbols C(i), i = 2, 3, ... , represent further proton configurations. Figures 2 and 3 present two pathways of proton configurations along which protons can be conducted. In the top pathway of Figs. 2 and 3 an excess proton enters the channel at the left-hand side, denoted by the transition C(1) = OX OX OX OX OX → C(2) = XX OX OX OX OX. The excess proton XX is then transported across the membrane by a series of N − 1 jumps between the groups, e.g., XX OX OX OX OX → OX XX OX OX OX. At the right side the excess proton is released into the solution, as described by the transition C(N + 1) = XO XO XO XO XX → C(N + 2) = XO XO XO XO XO, i.e., the conductor enters an equilibrium configuration. In the bottom pathway of Figs. 2 and 3, a proton jumps between the two central groups of the conductor and thereby creates a double fault of an excess proton XX and an empty group OO. These states correspond to the carboxylate anion of the aspartic acid and the hydronium-like ion on its neighboring residue. The excess proton XX wanders to the right-hand side where it will be given off to the solution. An excess proton then enters the conductor from the left-hand side and wanders to the center where it combines with the carboxylate anion.

These events leave the conductor again in the equilibrium configuration $C(N + 2)$.

In order to return the conductor for either pathway from $C(N + 2)$ back to the equilibrium configuration C(1), successive rotations or reorientations of the single groups are necessary. This part of the conduction is then common to both pathways. Since the transport in the top pathway of Figs. 2 and 3 involves the oxonium- and hydronium-like excess protons XX, so-called double-ionic faults D_t, this pathway has been labeled D_t. Since the conduction along the bottom pathway in Figs. 2 and 3 involves the simultaneous formation of a vacancy as well as an excess proton, the bottom pathway has been labeled L_tD_t.

Resistance of a Proton Channel

With small potential or pH differences across the membrane, a proton conductor operates near thermal equilibrium and, in analogy to Ohm's law, a linear relationship between the passive proton current and the applied chemiosmotic potential gradient (affinity) exists. For an application of the linear voltage–current relationship one has to consider the network of cycles contributing to the proton current. This may be illustrated for the network in Fig. 3. The network is composed of three unbranched segments, I, II, and III, such that I + II and I + III form the D_t and the L_tD_t cycle, respectively. If ΔV_I is the voltage decrement along segment I, then the flux along I is

$$J_I = R_I \Delta V_I$$

where[13,17]

$$R_I = (kT/e) \sum_{i \in M_I} 1/k_i^0 p_i^0 \tag{8}$$

Here M_I is the set of proton configurations of segment I, i.e., $M_I = \{C(1), C(2N + 1), \ldots, C(N + 3), C(N + 2)\}$, and p_i^0 and k_i^0 are the equilibrium ($\Delta V_I = 0$) probability and forward rate constant for configuration $i \in M_I$, e.g., $k_1^0 = k_{2n+1 \leftarrow 1}$. Similarly, one can evaluate the resistances contributed by the segments II and III. Following Kirchhoff's law, the resistance R of the complete network is

$$R = R_I + (R_{II}^{-1} + R_{III}^{-1})^{-1} \tag{9}$$

such that the total proton current J is

$$J = R\Delta V$$

where ΔV is the chemiosmotic potential applied across the conductor.

[17] J. Schnakenberg, *Rev. Mod. Phys.* **48**, 571 (1976).

Results

Figure 4 provides a comparison between the proton conductance $1/R$ as measured by Schindler and Nelson and as evaluated by means of Eqs. (8) and (9). R_0 scales the resistance and was set to the value 1/20 pS used by Schindler and Nelson. In the calculation we assume that the rate constants k_r for the rotation of the conductor groups are identical. The resistance for the rotational sequence has then the simple form $R_I = N/k_rP_r$ where P_r is the probability for the conductor to be found in a proton configuration containing at most one rotational fault. Agreement with the single-channel measurements at low pH is only possible if one assumes that the rate constant for the reorientation of a group is similar to that of water, $k_r \approx 10^{10}$ sec^{-1}. In this case, the resistance of the rotational sequence is negligible in comparison with the contributions from the jumps and the protonation processes. The necessity of fast rotations of the conductor groups implies that the hydrogen bonds between the conductor groups are weak and is consistent with a model of the proton channel constructed from molecules of bound water and perhaps flexible amino acid side groups such as threonine. Furthermore, it implies that amino acid side groups with bulky aromatic rings are probably not involved in the proton transport in the proteolipids.

Due to aggregation of the proteolipids, Schindler and Nelson could only measure at higher pH values the total conductances and not the conductance from a single proton channel, so that a discrepancy from our single-channel results is to be expected. However, part of the observed increase could be due to the change in the conduction pathway. At very acidic pH, the conduction occurs primarily with the transport of an excess proton (the D_t cycle of Fig. 3). At pH values greater than the pK of

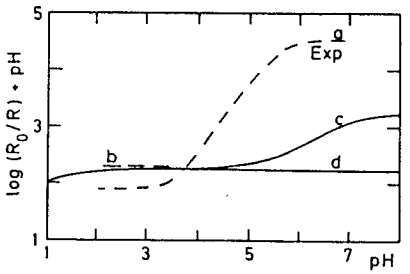

FIG. 4. pH dependence of the conductance $\Lambda = 1/R$ predicted for a single proton channel and as observed by Schindler and Nelson[4]: The scale factor for the resistance is $R_0 = 1/20$ pS, the applied voltage difference is $V = 50$ mV. (a) Total conductance observed; (b) single-channel conductance extrapolated from Ref. 4; (c, d) theoretical predictions for a channel with $N = 11$ groups, with the protonation rate constant (κ_d) in Eq. (3) increased fourfold; (d) contribution of the D_t cycle alone (see Fig. 2).

aspartic acid, the cycle involving the migration of a vacancy (the L_tD_t cycle of Fig. 3) dominates the conductance. However, the single-channel proton current in this pH range cannot be observed and hence, the direct involvement of aspartic acid in the proton channel cannot be proved. At low pH, aspartic acid behaves very much like water, since the respective pK_2 values are similar. Hence, it is entirely possible that the proton channel connected with the proteolipids of ATPase entails solely molecules of water as conductor groups.

Titration of a Stationary Proton Current[13]

In this section we want to demonstrate how a measurement of the pH dependence (titration) of a stationary proton current induced by a fixed voltage difference can yield information on the pK values of the conductor groups. For this purpose we present in Fig. 5 the dependence of the stationary proton current through a homogeneous conductor on the conducting group's pK and on pH. The current has been evaluated by means of Eq. (4). At low pH the proton transport involves a single cycle of sequential proton configurations. This cycle corresponds to the (upper) D_t cycle in Figs. 2 and 3. A first part of this cycle involves proton configurations which describe the migration of an excess proton (D_t fault) through

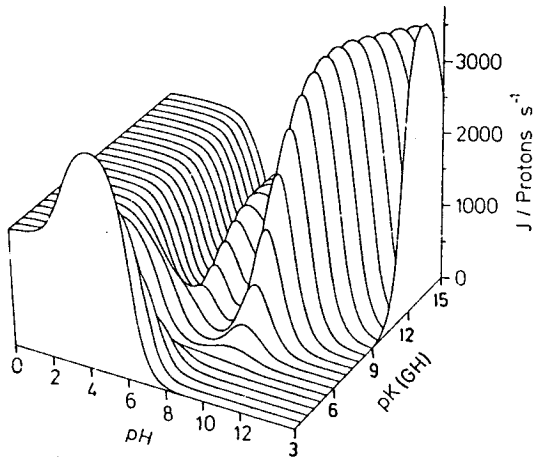

FIG. 5. Stationary proton current across a homogeneous chain of $N = 4$ side groups capable of accepting two protons as a function of pK(XH) with p$K(XH_2) = -2$ and as a function of $pH = pH_a = pH_b$. The current is induced by an external electrical potential $\Delta V = 100$ mV.[13]

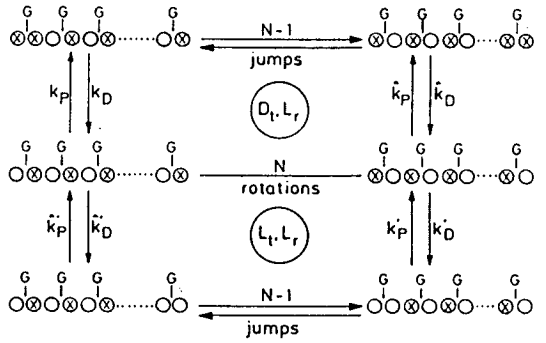

FIG. 6. The (D_t, L_r) and (L_t, L_r) single-file cycles.

the conductor. The following part of the cycle involves those configurations which correspond to a deprotonation and the return of the conductor to its starting configuration by successive rotations of the side groups (L_r fault migration). The described (D_t, L_r) cycle is shown in Fig. 6. As the pH increases the contribution of the D_t, L_r cycle diminishes, and the proton conduction takes place through a second cycle which involves the migration of a vacancy (L_t fault) in the opposite direction. This cycle, also presented in Fig. 6 differs from the L_tD_t cycle in Fig. 2 in that a single fault (L_t = OO) is created at the conductor end, whereas the bottom cycle in Fig. 2 involves a double fault (D_tL_t = OO XX) which is created at the center of the cycle. The transport mechanism in Fig. 6 can be tested by a titration experiment in which a proton current at various pH values is observed. A comparison of an observed proton current with the calculated current shown in Fig. 5 should allow one to determine the pK values of the conductor groups. In fact, such an experiment has been performed on the proton channels formed by the proteolipids of ATPase. However, in this case the pH range over which single-channel proton conductance could be observed was too narrow to exhibit the transition between the two conduction cycles.

Proton Diodes[13]

Proton conduction across energy-transducing membranes often has a distinct vectorial character. Hence, the energy transduction would function best if the underlying proton conductors obey a diodic voltage–current characteristic. To achieve this property the proton conductor has to be necessarily heterogeneous. The heterogeneity can be achieved by the participation of heterogeneous (acidic and basic) side groups, by the pres-

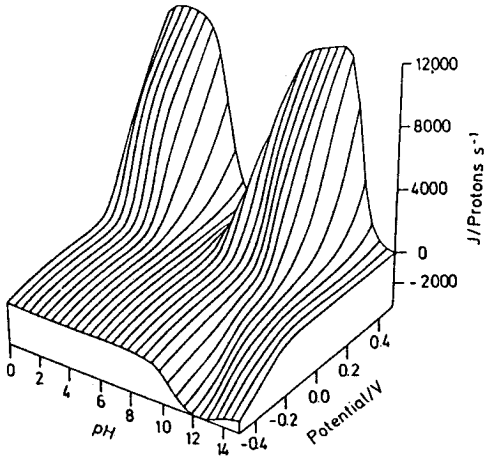

FIG. 7. Proton diode. The stationary proton current across a "field diode" as a function of the applied voltage and solution pH. The field diode is constructed from a homogeneous conductor possessing an internal electric field of V_{int} = 300 mV across the chain. The four groups in the homogeneous conductor are characterized by the pK values, pK(GH) = 10 and pK(GH_2) = −2.[13]

ence of internal electric fields, or by a combination of the two. Although we have performed calculations on both types of diodic conductors,[13] we will discuss here only the case of a proton diode realized for a homogeneous chain through an internal field (field diode). The internal field can arise through dipoles aligned along the conductor. Edmonds[18] has suggested that a water channel spanning a biomembrane could conduct ions vectorially if the dipoles of the water molecules were properly oriented. Proteins alone could achieve an internal field through the dipole moments of polar side groups or through the dipole moments of the peptide backbone [illegible]ard to the latter possibility, it is of interest to observe that bacte[illegible]opsin is composed of seven α-helices spanning the outer membra[illegible] H.h. Since consecutive helices are oppositely directed, one expects [illegible]the dipole moments of six α-helices cancel and the dipole moment o[illegible]eventh helix remains. Since the NH-terminal end is located at the extra[illegible]llular side, the residual dipole moment should be oriented against the p[illegible]ton transport in the pump cycle. This orientation may be in harmony with the observation that the initial charge displacement in bacteriorhodopsin is against the pump direction. Several groups[19] have reported that bacteriorhodopsin has a permanent dipole moment with a value ranging from 70 to 100 debyes.

[18] D. Edmonds, *Chem. Phys. Lett.* **65**, 429 (1979).

[19] See, for example, K. Barabas, A. Dér, Zs. Dancshazy, P. Ormos, L. Keszthelyi, and M. Marden, *Biophys. J.* **43**, 5 (1983).

The stationary proton current along a homogeneous chain with an internal field of 300 mV is shown in Fig. 7 as a function of the applied voltage and of the solution pH. The internal field assumed is linear with a zigzag profile, the free energy being 150 mV above the solution at side a, falling off linearly to a free energy 150 mV below the solution at side b. The chain consists of groups able to accept two protons. The internal field modifies the pK values so that the end group at side a has lower effective pK values than the end group at side b. The figure demonstrates that the field diode gives rise to a larger proton current in the forward direction than in the reverse direction.

Buffering Capacity and Refractory Phase of Proton Conductors[13]

In this section we consider the proton transport from the active site to the extracellular side (from the intracellular side to the active site) of bacteriorhodopsin. For this purpose we connect a proton conductor to an acid (base) with the capability to inject a proton into (remove a proton from) the conductor. Allowing the interaction between the proton conductor and the injecting (ejecting) group to be time dependent, we investigate the refractory phase that exists after an initial proton current pulse and demonstrate the buffering capacity of the conductor—a function that we associate with the *blue light effect* in bacteriorhodopsin.

In bacteriorhodopsin the injecting group could be its chromophore, a protonated Schiff base of all-*trans*-retinal. According to a mechanism proposed in Refs. 20 and 21, the absorption of light by bacteriorhodopsin in its Br_{568} state induces an isomerization to a twisted 13-*cis* conformation which includes a 14s-*cis* rotation and which leaves the chromophore in the L_{550} intermediate acidic with respect to the proton conductor groups. The Schiff base proton can then be injected into the conductor in contact with the extracellular space, transferring bacteriorhodopsin thereby to the M_{412} intermediate state. At room temperature the M_{412} intermediate with an unprotonated 13-*cis*-retinal chromophore returns through a series of intermediates within milliseconds to its original Br_{568} state with a protonated all-*trans* chromophore. The reaction cycle involves the transport of 1–2 protons. However, through irradiation of the M_{412} intermediate the Br_{568} intermediate can already be reached within 10^{-9} sec. This fast reaction

[20] K. Schulten and P. Tavan, *Nature (London)* **272**, 85 (1978).

[21] K. Schulten, Z. Schulten, and P. Tavan, *in* "Information and Energy Transduction in Biological Membranes" (L. Bolis, E. Helmreich, and H. Passow, eds.). Liss, New York, 1984; P. Tavan, K. Schulten, and D. Oesterhelt, *Biophys. J.* **47**, 415 (1985); see also P. Tavan, K. Schulten, *Biophys. J.*, in press (1986).

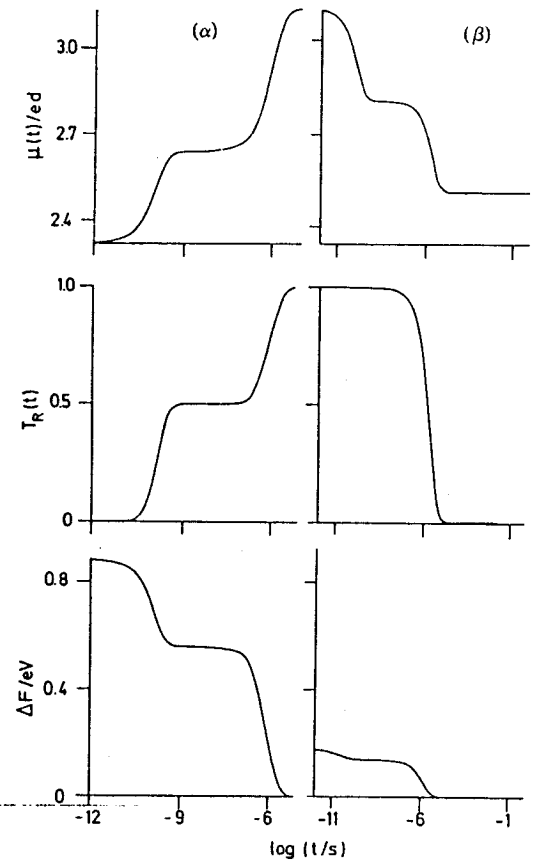

FIG. 8. Blue light effect on bacteriorhodopsin: The pK values of the conductor groups are pK(XH) = 10, pK(XH_2) = −2, and the injector pK(inj) = −4. The solution at the right (see Fig. 1) is at pH_b = 7. (α), At t = 0 the protonated injector is coupled to the conductor; (β), at $t = 10^{-5}$ sec a sudden increase in the injector pK value occurs, to pK(inj) = 10. Presented are the dipole moment $\Delta\mu(t) = \mu(t) - \mu(0)$, the integrated proton current $T_R(t)$, and the change in free energy $\Delta F(t)$.[13]

route does not involve a net transport of protons, which suggests that M_{412} after light excitation increases its pK, attracts the proton given off at the L_{550} stage back from the conductor, and then reisomerizes to the all-*trans* chromophore.

A crude simulation of this so-called *blue light effect* is presented in Fig. 8. At t = 0, a protonated injector group with pK = −4 representing the retinal chromophore at the L_{550} stage is coupled to a homogeneous

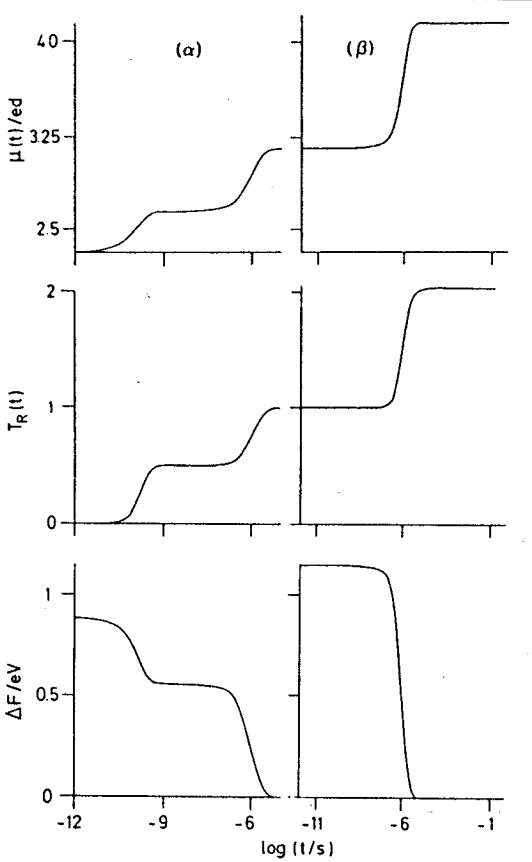

FIG. 9. Refractory phase: Demonstration of the delay time of the homogeneous conductor in Fig. 8. (α) At t = 0 a protonated injector group is coupled to the conductor; (β) at $t = 10^{-5}$ sec a new protonated injector group is brought into contact. The calculated quantities are defined in Fig. 8.[13]

conductor which establishes the proton pathway of bacteriorhodopsin from the chromophore to the extracellular side. The irradiation with blue light at $t = 10^{-5}$ sec is assumed to cause an instantaneous change in the injector's pK from −4 to 10, representing M_{412} in the excited state. The injector then abstracts a proton from the conductor end group and creates a vacancy (L_t fault) within the conductor. This vacancy moves to the extracellular conductor end within 10^{-9} sec. Reprotonation and reorientations of the conductor groups return the system to its original equilibrium

configuration. Our calculation, represented in Fig. 8, shows the following behavior: As indicated by the change in the dipole moment $\mu(t)$, the integrated current $T_R(t)$ across the extracellular end group and the change in free energy $\Delta F(t)$, once the acidic injector gives off the proton to the conductor, it is translocated to the solution within 10^{-6} sec. However, light excitation, which renders the injector basic, induces a decrease of the conductor's dipole moment within 10^{-9} sec. After about 1 μsec, the conductor is reprotonated at the extracellular side, as indicated by the current, and returns to its equilibrium. In our simulation the dipole moment does not return to its exact original value, since we left the basic injector group in contact with the conductor.

At room temperature and neutral pH, the photocycle of the proton pump in bacteriorhodopsin requires milliseconds to return to its original state. It is of interest to see whether another proton could be conducted before the conductor has equilibrated. For this purpose we assume that 10^{-5} sec after the injection of a first proton into a channel, a new protonated injector group is brought into contact with the channel. Figure 9 shows the result for such a situation. Until $t = 10^{-5}$ sec the behavior of the system is the same as in Fig. 8 (different scaling). Anewed protonation at $t = 10^{-5}$ sec of the injector group results in a state of high free energy. However, Fig. 9 shows that the system has to await the migration of a D_r rotational fault before ($t \approx 10^{-6}$ sec) the second proton is accepted and conducted by the channel. The time period lasting 10^{-6} sec has to be interpreted as a refractory phase during which the conductor groups need to rotationally relax before anewed conduction can occur.

Response to Oscillating Fields[13]

Measurement of the charge displacements within bacteriorhodopsin and field jump experiments on this protein record the motion of all charges within the protein and not just those involved in the proton conduction. If the protonation and deprotonation processes at the channel entrance are rate determining, measurement of the proton current will also not reveal information of the conductor groups. In a preliminary effort to find suitable "windows" for the elementary conduction processes, we have calculated the response of proton conductors to oscillating electric fields. By varying the field frequency and the solution pH, the desired separation of the transport processes can be achieved for model systems.[13]

Figure 10 depicts the dipole moment induced in a homogeneous conductor by an oscillating field $V\sin(2\pi\nu t)$ of variable frequency ν. Both ends of the conductor are assumed in contact with an aqueous solution at

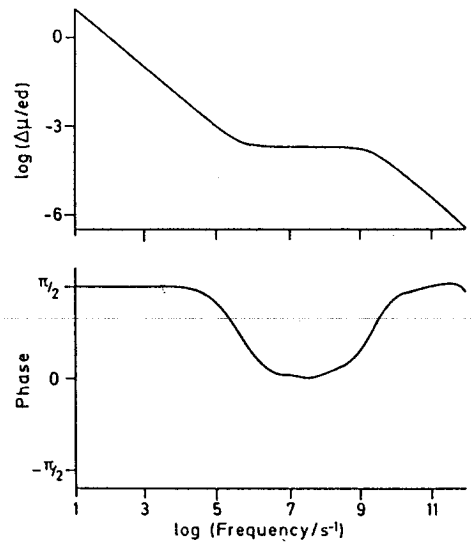

FIG. 10. Response to an oscillating field: Frequency dependence of the dipole moment $\Delta\mu$ and the proton current ΔJ of a homogeneous conductor at pH 7 in an alternating electric field with amplitude V_{ext} = 25 mV. The conductor is the same as in Fig. 8.[13]

pH = 7. At frequencies below 10^5 Hz, the dipole moment $\Delta\mu$ (defined as the difference between the largest and the smallest value of μ during a cycle of the external field) is due to a net proton transport across the conductor involving protonation and deprotonation processes at the conductor ends. In this frequency range the proton flux J_R at the ends is linear with the external field and the dipole moment is

$$\Delta\mu \sim \int_0^{\pi/\omega} J_R\, dt \sim \int \sin \omega t\, dt \sim \omega^{-1}$$

i.e., decreases inversely with the frequency. This behavior is clearly reflected in Fig. 10. The phase of $\Delta\mu$ is determined by the integral

$$\int_0^t J_R\, dt \sim \int_0^t \sin \omega t\, dt \sim \cos \omega t$$

i.e., the phase shift relative to the external field measures $\pi/2$. At 10^5 Hz the protonation–deprotonation reactions at the conductor ends cease to follow the oscillating external field. The diplole moment change is then solely due to the shuttling of charges carried by D_t, L_t, D_r, and L_r faults within the conductor through proton jumps and group rotations. In the

range 10^7 Hz $< \nu < 10^9$ Hz the migration of an L_t fault across the conductor determines $\Delta\mu$ and follows adiabatically the external field. Hence, the phase of $\Delta\mu$ vanishes and $\Delta\mu$ itself assumes a stationary value. At frequencies above 10^9 Hz the internal charge motion cannot follow the field adiabatically. The dipole moment $\Delta\mu$ decreases and assumes again the phase shift $\pi/2$. The behavior shown in Fig. 10 depends sensitively on the mechanism of proton transport, i.e., on the proton configurations involved. For example, at pH = 10 when the conduction shifts to the L_tL_r mechanism (see above), the frequency dependence of $\Delta\mu$ and its phase shift change considerably from the behavior just discussed and reflected in Fig. 10. Yet another frequency behavior is predicted for the proton diodes. Hence, we suggest that the response of conductors to oscillating fields can be employed to characterize biological proton transport and to detect proton diodes in biological systems. Frehland and Faulhaber[22] have studied the frequency dependence of biological ion transport. They have shown that the internal structure of the ion pores (e.g., the barrier heights and the number of binding sites) has an influence on the frequency dependence of the macroscopic admittance and current.

Outlook

Unlike ionic conductivity in solids, proton currents in biological systems involve only a small percentage of the atoms composing the system, and unlike the static hydrogen-bonded network that stabilizes the α-helix structure, the bonds in the proton conductors are constantly being broken by reorientation of the conducting groups. These two aspects of the biological proton transport make its detection exceedingly difficult. The constituents of a biological proton conductor are most likely molecules of bound water or the polar amino acid side groups of the protein. The molecular dynamics calculations on the ion channel in gramicidin indicate that a linear water channel may be the conducting pathway in ion channels as well. The participation of polar amino acid side groups that are embedded within the membrane is more difficult to detect. Blocking or altering groups thought to be participating is one of the few direct methods. Our calculations show that titration of stationary proton currents and observations of responses to time-dependent electric fields at various pH values should reveal the pK values of the conducting groups and indicate whether the conductor is heterogeneous or homogeneous. Once high-resolution structures of proton-transporting proteins are obtained, molecular dynamics simulations may provide further details of the conduction mechanism.

[22] E. Frehland and K. H. Faulhaber, *Biophys. Struct. Mech.* 7, 1 (1980).